

Supplementary Information

***APOE4* causes widespread molecular and cellular alterations associated with Alzheimer's disease phenotypes across human iPSC-derived brain cell types**

Yuan-Ta Lin, Jinsoo Seo, Fan Gao, Heather M. Feldman, Hsin-Lan Wen, Jay Penney, Hugh P. Cam, Elizabeta Gjoneska, Waseem K. Raja, Jemie Cheng, Richard Rueda, Oleg Kritskiy, Fatema Abdurrob, Zhuyu Peng, Blerta Milo, Chung Jong Yu, Sara Elmsaouri, Dilip Dey, Tak Ko, Bruce A. Yankner and Li-Huei Tsai

Figure S1.

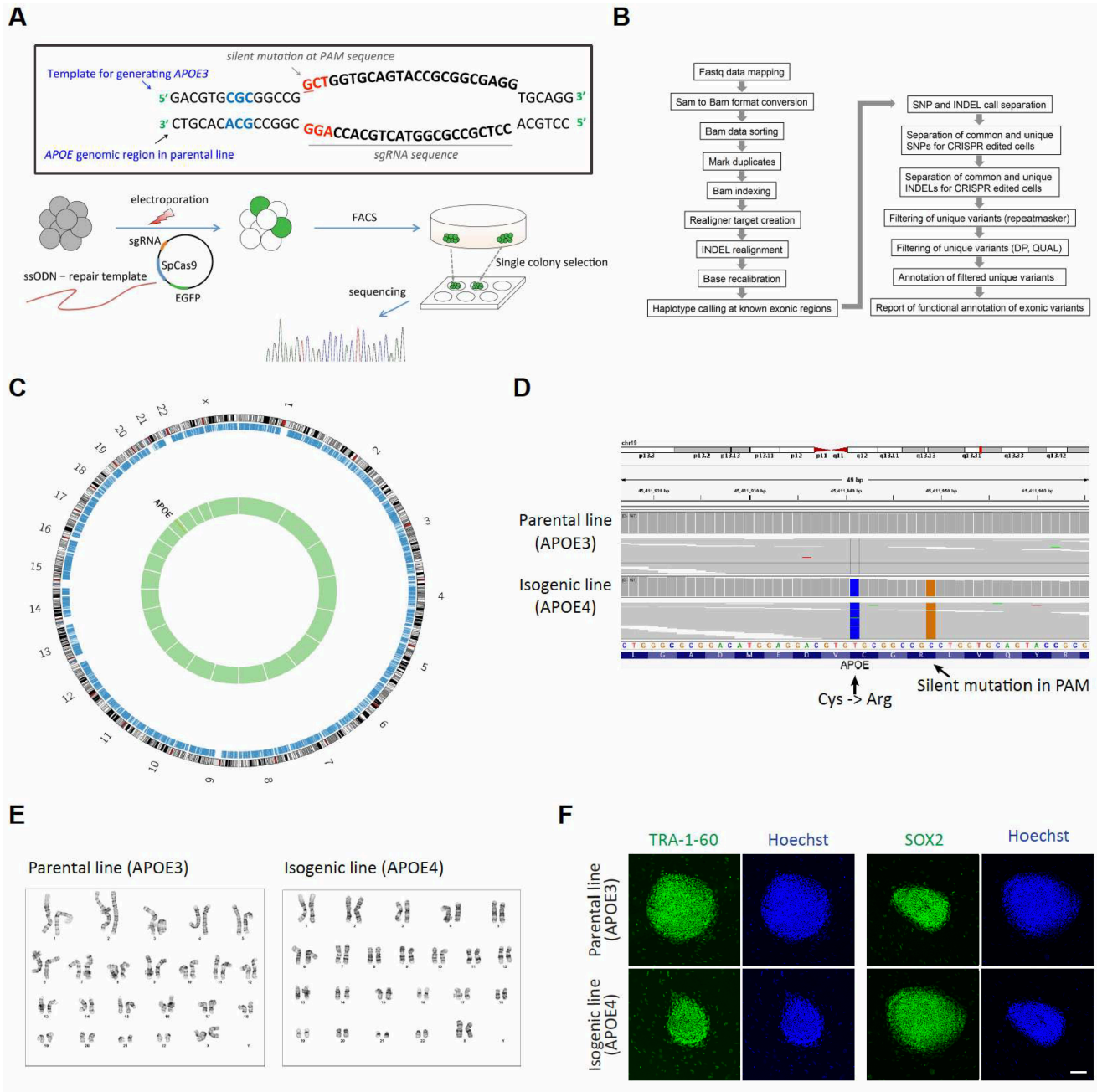


Figure S1 (Related to Figure 1). Generation of isogenic *APOE4* iPSCs.

(A) Schematics for CRISPR/Cas-9 genome editing. We designed a sgRNA targeting *APOE* gene near Cys112 coding region. Then, this sgRNA was integrated into a plasmid containing *S. pyogenes*-Cas9 coding gene and EGFP sequence. As a repair template, ssODN was designed to carry 200 nucleotides including coding sequence for Arg112 instead of Cys112, and silent mutation at PAM site to prevent additional DNA breaks in edited cells. iPSCs were electroporated to introduce the plasmid along with ssODN, and then only GFP-positive, Cas9-expressing cells were collected by FACS. Cells were then plated sparsely to allow single-cell colony formation. Each colony was inspected by Sanger sequencing to investigate whether Cys112 coding sequence was correctly replaced with Arg112 sequence.

(B) The pipeline for whole exome sequencing data to inspect potential off-target insertion/deletion or single nucleotide variation (SNV) by CRISPR/Cas9 genome editing.

(C) The genomes represented as concentric circles to show differential nucleotide sequence in isogenic *APOE4* iPSCs compared to parental *APOE3* iPSCs. The black outer ring depicts the human chromosomes and the blue ring represents a map of gene densities. The green ring indicates variant display background, and variant location (only *APOE* gene) shown as red-color line in the green circle.

(D) The genome browser shows two SNVs, *APOE3/4* coding locus and silent mutation insertion in PAM, in *APOE* gene of isogenic *APOE4* iPSCs compared to parental *APOE3* iPSCs.

(E) Both isogenic and parental iPSCs have normal karyotypes.

(F) Immunocytochemistry with TRA-1-60 and SOX2 antibodies in isogenic *APOE4* iPSCs and parental *APOE3* iPSCs. Scale bar = 80 μ m.

Figure S2.

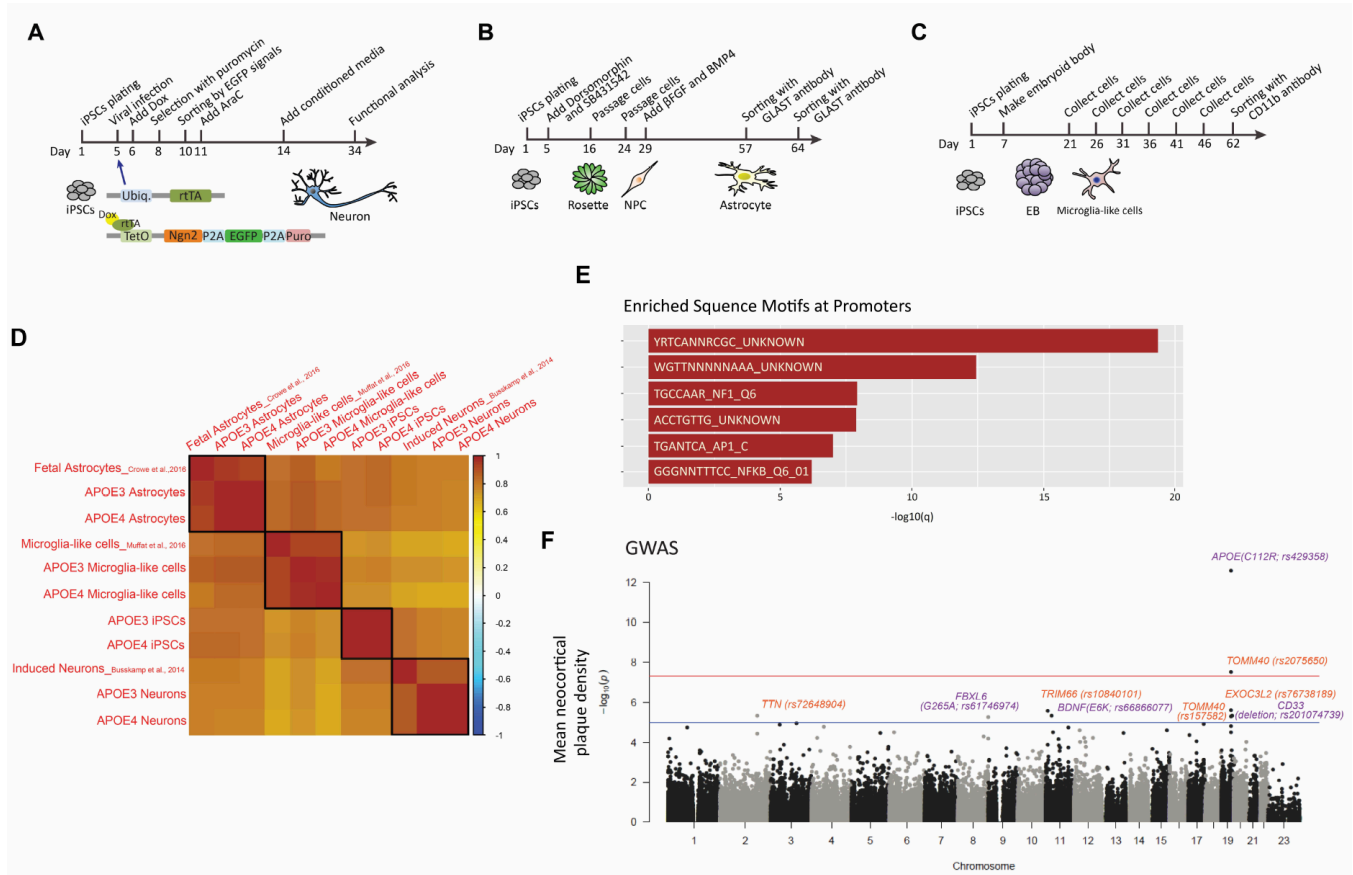


Figure S2 (Related to Figure 1). Generation of neurons, astrocytes and microglia-like cells from isogenic iPSCs carrying either *APOE3* or *APOE4* alleles.

(A-C) Schematics for generating iPSC-induced neurons, astrocytes and microglia-like cells.

(D) Hierarchical clustering of RNA-seq data from iPSC-derived neurons, astrocytes and microglia-like cells carrying either *APOE3* or *APOE4* together with publicly available cell type specific RNA-seq data from other groups (see methods). Color scale represents Pearson's correlation coefficient.

(E) Genome-wide association of SNP variants identified from human brain exome-seq data with phenotypic mean neocortical plaque density. SNP variants with p-value < 1E-5 are highlighted. Nonsynonymous variants are colored in purple.

Figure S3.

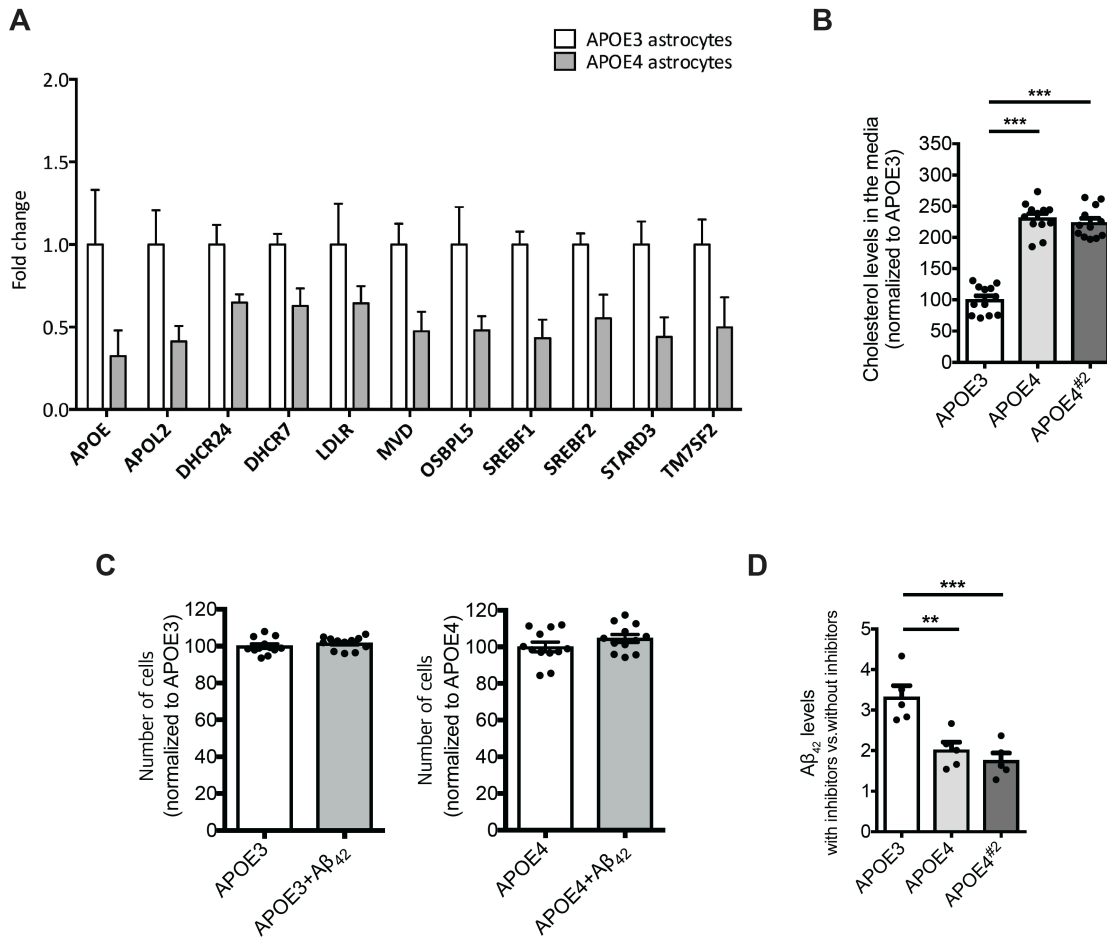


Figure S3 (Related to Figure 3). Altered lipid metabolism and impaired lysosome-dependent Aβ degradation in *APOE4* astrocytes compared to *APOE3* astrocytes.

(A) Decreased genes in the category of 'cholesterol/sterol metabolism and transport' by GO analysis in *APOE4* astrocytes (n=3, fold change: *APOE4* vs *APOE3*, $q < 0.05$, error bars \pm s.e.m.). (B) Extracellular cholesterol levels were measured in media from two independent *APOE4* isogenic astrocyte cultures and *APOE3* astrocyte cultures. n=12 from three independent cultures. (C) Number of cells in *APOE3* and *APOE4* astrocytes followed by Aβ₄₂ treatment (250 ng/ml for 2 days). n=12 from three independent cultures. (D) Lysosome-dependent Aβ₄₂ degradation in astrocytes induced from two independent *APOE4* iPSC clones and *APOE3* iPSC. n=5 from two independent cultures.

(** $P < 0.01$, *** $P < 0.001$ by Dunnett's test; error bars \pm s.e.m.)

Figure S4.

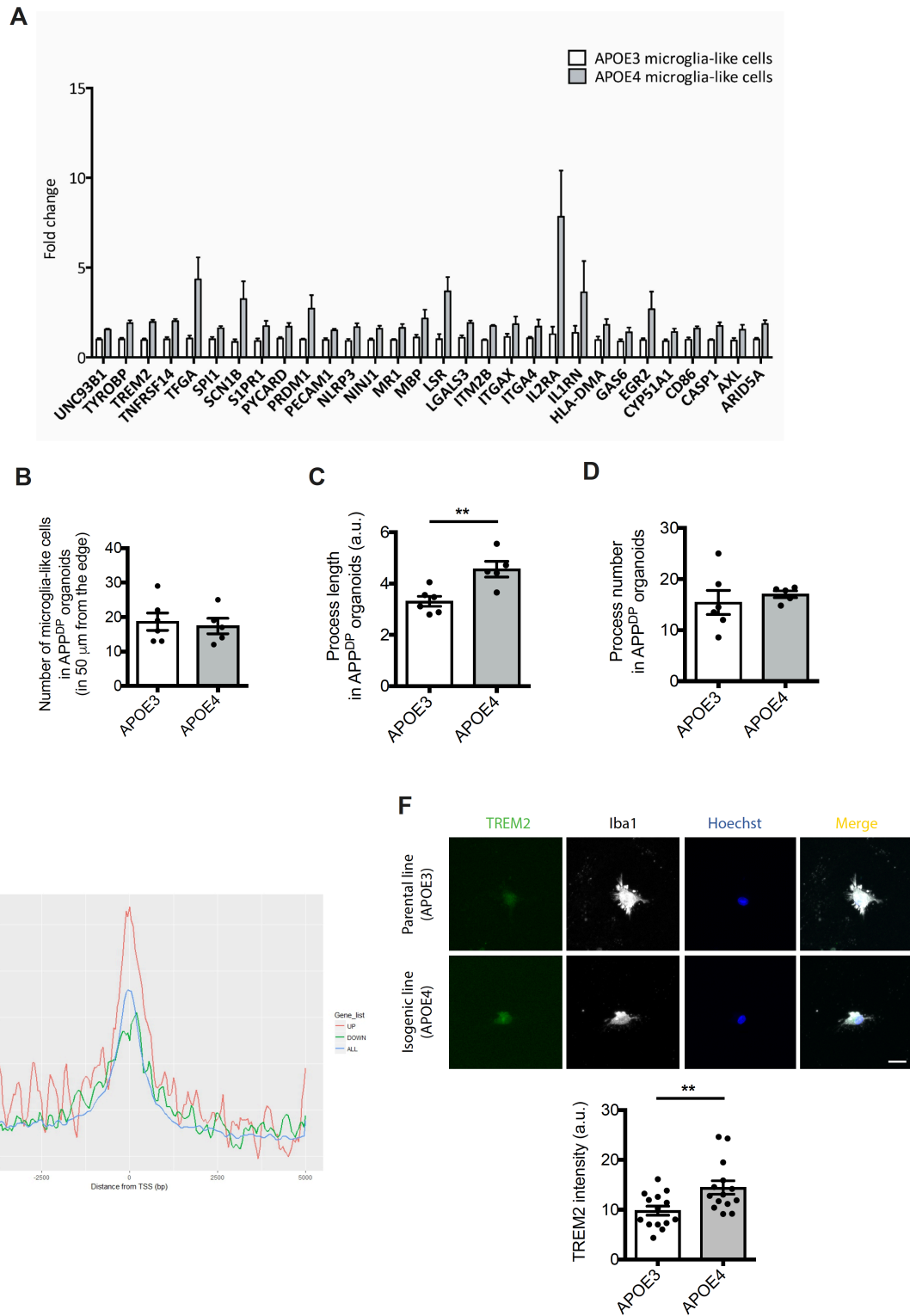


Figure S4 (Related to Figure 4). Pathological features in *APOE4* microglia-like cells.

(A) Increased genes in the category of 'inflammation of central nervous system' by Ingenuity Pathway Analysis in *APOE4* microglia-like cells (n=4, fold change: *APOE4* vs *APOE3*, $q < 0.05$, error bars \pm s.e.m.). (B) Number of microglia-like cells incorporated into *APP^{DP}* organoids. n=5~6 organoids. (C, D) Process length and number of microglia-like cells in *APP^{DP}* organoids were examined by immunocytochemistry with Iba1 antibody. n=5~6 organoids. (E) Aggregation plot of average Irf8 ChIP-Seq intensity signals around gene transcription start sites (TSS). Average signals for mouse ortholog sets of up- and down-regulated genes in *APOE4* microglia-like cells were compared. Signals for all mouse annotated genes were also included in the plot. (F) Immunocytochemistry with TREM2 and Iba1 antibody in *APOE3* or *APOE4* microglia-like cells. Bar graphs represent relative immunoreactivity of TREM2 in *APOE3* or *APOE4* microglia-like cells. n=14 from three independent cultures. Scale bar = 20 μ m.

(** $P < 0.01$, by Student's t-test; error bars \pm s.e.m.)

Figure S5.

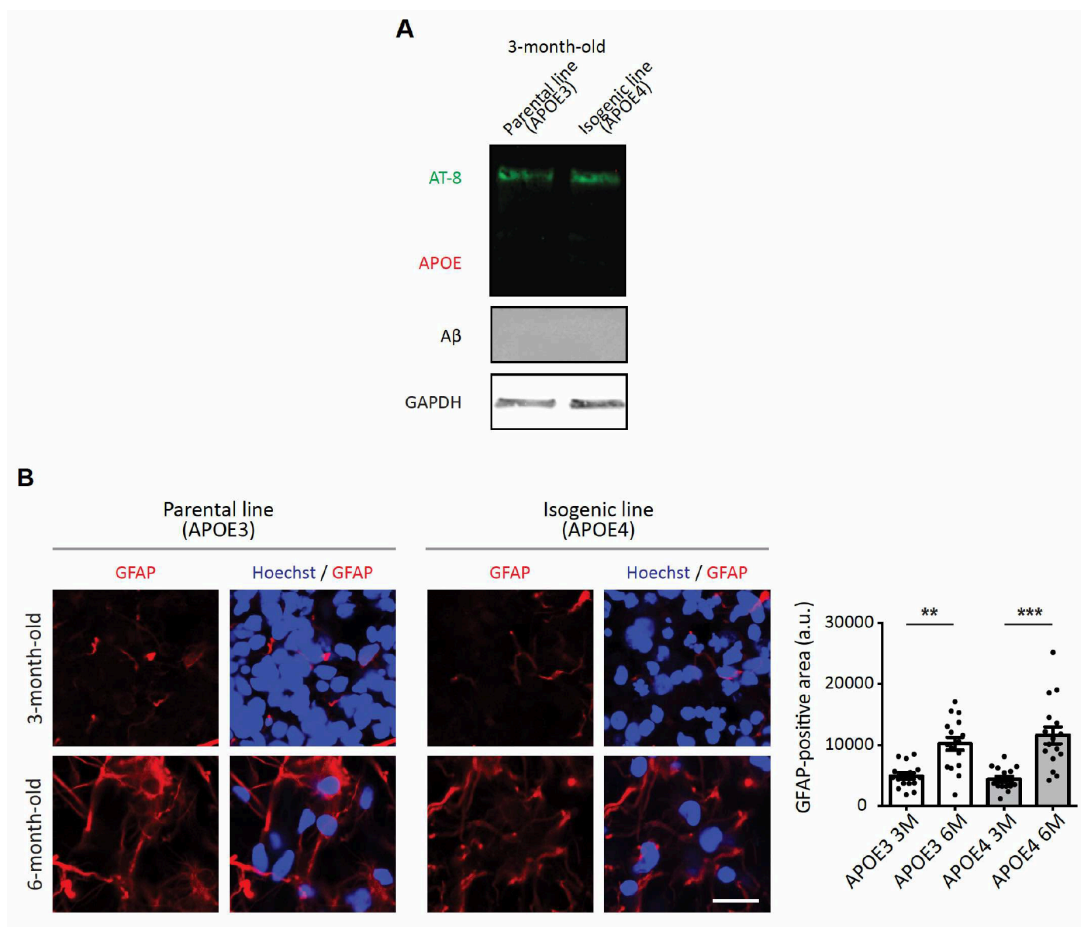


Figure S5 (Related to Figure 5). Increased GFAP-positive cells with age in iPSC-induced cerebral organoids.

(A) Three-month-old organoids from *APOE3* or *APOE4* iPSCs were lysed and subjected to the immunoblotting with antibodies against APOE, A β , AT-8 or GAPDH.

(B) Three-month and six-month-old organoids from *APOE3* or *APOE4* iPSCs were fixed and subjected to the immunostaining with GFAP antibody. A bar graph represents relative immunoreactivity of GFAP in organoids. Scale bar = 20 μ m. n=16 images from 4~6 organoids.

($P < 0.0001$ by ANOVA, $**P < 0.01$, $***P < 0.001$ by Tukey's test; error bars \pm s.e.m.)

Figure S6.

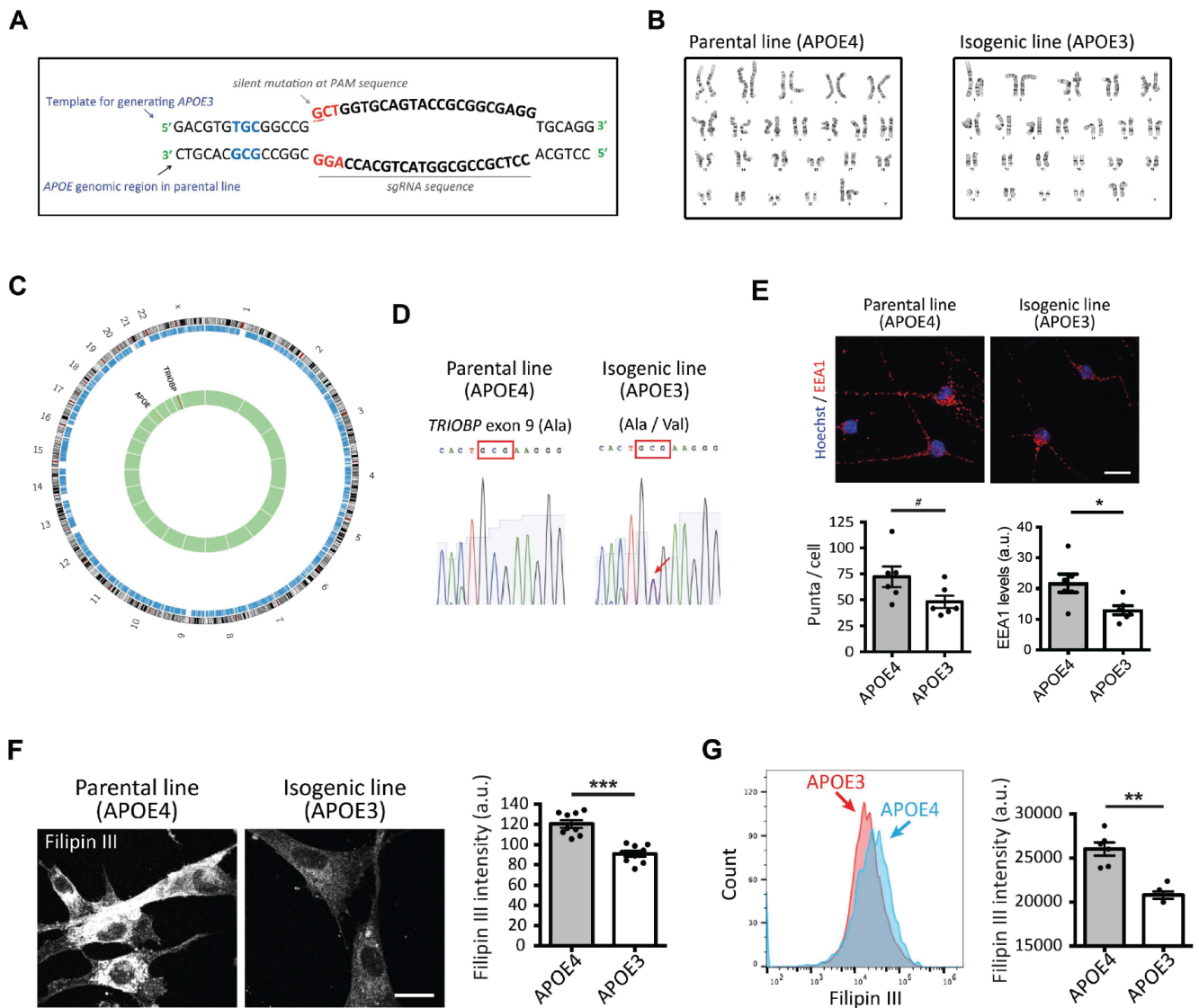


Figure S6 (Related to Figure 6). Converting *APOE4* to *APOE3* attenuates AD-related phenotypes in sAD iPSC-induced neurons, glia and organoids.

(A) The sequence of sgRNA and ssODN to generate isogenic *APOE3* iPSCs from sAD iPSCs carrying *APOE4* alleles.

(B) Both isogenic and parental iPSCs have normal karyotypes.

(C) The genome represented as concentric circles to show differential nucleotide sequence in isogenic *APOE3* iPSCs compared to parental *APOE4* iPSCs. The black outer ring depicts the human chromosomes and the blue ring represents a map of gene densities. The green ring indicates variant display background, and variant location (*APOE* and *TRIOBP* gene) shown as red-color line in the green circle.

(D) The variant in *TRIOBP* gene occurred in one allele and potentially results in replacement of the nonpolar Ala with nonpolar Val in exon 9.

(E) Immunocytochemistry with EEA1 antibody in iPSC-derived neurons from *APOE4* or *APOE3* iPSCs. Scale bar = 10 μm . n=6 from three independent cultures.

(F) iPSC-derived astrocytes were fixed and incubated with filipin III for 1hr followed by imaging. Scale bar = 10 μm . n=9 images from three independent cultures.

(G) iPSC-derived astrocytes were sorted based on the intensity of filipin III. n=3~6 per group.

(# $P=0.06$, * $P<0.05$, ** $P<0.01$, *** $P<0.001$ by Student's t-test; error bars \pm s.e.m.)